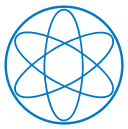

Technical University Munich
Physics Department

Max Planck Institute for Physics
Werner Heisenberg Institute

Advanced Lab Course

Neutrino Mass Analysis with KATRIN

Christian Karl, Susanne Mertens, Martin Slezák

Last edited: October 27, 2022

Contents

Chapter 1

Introduction

The neutrino was postulated in 1930 by Wolfgang Pauli to describe the continuous electron energy spectrum observed in β-decay experiments. Over 20 years later, in 1956, it was experimentally confirmed by the Cowan-Reines neutrino experiment [1].

Since its discovery the understanding of the neutrino has increased tremendously and it is now well embedded in the Standard Model of particle physics. Neutrinos participate in the weak interaction, one of the three fundamental forces described by the Standard Model and the one responsible for β-decay. In correspondence with the charged leptons, the electron, the muon and the tau, neutrinos come in three different flavours.

Various experiments have proven that it is possible for neutrinos to change their flavour by neutrino oscillations [2–4]. Neutrino oscillations arise from the fact that neutrino mass eigenstates are not equal to neutrino flavour eigenstates. Each flavour is composed of the three different mass states with a unique mixing described by the Pontecorvo-Maki-Nakagawa-Sakata (PMNS) matrix (1.1) [5, 6]. Differences in mass lead to a different propagation of the mass state components through space.

$$\begin{pmatrix} \nu_e \\ \nu_\mu \\ \nu_\tau \end{pmatrix} = \begin{pmatrix} U_{e1} & U_{e2} & U_{e3} \\ U_{\mu 1} & U_{\mu 2} & U_{\mu 3} \\ U_{\tau 1} & U_{\tau 2} & U_{\tau 3} \end{pmatrix} \begin{pmatrix} \nu_1 \\ \nu_2 \\ \nu_3 \end{pmatrix} \tag{1.1}$$

The probability to oscillate from one state i into another state j

$$P_{i \to j} \propto \sin^2 \left(\frac{\Delta m_{ij}^2 L}{4E} \right) \tag{1.2}$$

shows that neutrino oscillation experiments are only sensitive to the difference of the squared masses of two different mass states $\Delta m_{ij}^2 = m_i^2 - m_j^2$. The existence of neutrino oscillations hence proves that neutrinos have mass, however the absolute mass scale of the neutrinos cannot be deduced from oscillation experiments.

Three methods to determine the absolute neutrino mass scale are currently being explored: cosmological investigation of large scale structure (LSS) formation and evolution [7], the search for neutrinoless double β-decay ($0\nu\beta\beta$) [8] and the analysis of the shape of the energy spectrum of electrons emitted by β-decay near the endpoint.

While the LSS analysis depends heavily on the cosmological model being used and $0\nu\beta\beta$ requires the neutrino to be a Majorana particle, the kinematics of β-decay do not depend on the neutrino mass model and are based on well-known physics. The **KA**rlsruhe **TRI**tium **N**eutrino (KATRIN) experiment is designed to explore the absolute neutrino mass scale using this method with unprecedented sensitivity.

In this data analysis course we will first understand the basic model the KATRIN experiment. Equiped with this, we can then investigate how the absolute value of the neutrino mass impacts the β-decay spectrum and thus how KATRIN attempts to infer its value. Finally we will come to the concepts of interval and uncertainty estimation as well as the idea of the sensitivity of an experiment.

To this end, the lab course is divided in three main parts:

1. The first part of the lab course focuses on the KATRIN experiment. Here your task will be to program a simplified model of the tritium β-decay spectrum and to graphically illustrate the impact of the neutrino mass on the shape of the spectrum. You will then implement KATRIN-specific experimental effects (such as energy resolution) in your model.

2. In the second part you will focus on data-analysis: You will learn how to infer the physics parameter of interest, in our case the neutrino mass, from a fit to the data. You will also learn how to correctly evalute the uncertainty of the fit result and set an upper limit in case no neutrino mass is found.

3. The acquired knowledge will then be applied to the actual data of the first physics run of the KATRIN experiment. You will repeat the analysis and set the world-leading limit on the neutrino mass from a direct neutrino-mass experiment yourself.

Chapter 2

The KATRIN Experiment

The **KA**rlsruhe **TRI**tium **N**eutrino (KATRIN) experiment is a next generation tritium β-decay experiment following the measurement principle of its predecessors in Mainz [9] and Troitsk [10]. It is designed to measure the effective electron anti-neutrino mass

$$m_\nu = \left(\sum_{i=1}^{3} |U_{ei}|^2 \cdot m_i^2 \right)^{\frac{1}{2}} \tag{2.1}$$

with a sensitivity of 200 meV [1] at 90 % confidence level (C.L.).

This chapter gives an overview of the measurement principle of the KATRIN experiment with a focus on deriving a model used for analysis. Much more details on the experimental setup can be found in the KATRIN design report [11], the model builds upon [12].

2.1 Neutrino Mass Determination from Beta-Decay

In a β^--decay process a neutron in a nucleus X is transformed into a proton leaving over the daughter nucleus Y and emitting an electron e^-, an electron anti-neutrino $\bar{\nu}_e$ and the surplus energy Q:

$$X \rightarrow Y + e^- + \bar{\nu}_e + Q. \tag{2.2}$$

The released energy Q is shared between the decay products. The daughter nucleus Y is left with the recoil energy E_{rec} while the remaining energy, called the endpoint E_0, is split between the electron and the anti-neutrino with corresponding energies E and E_ν respectively:

$$E_0 = Q - E_{\text{rec}} = E + E_\nu \tag{2.3}$$

As the energy of the neutrino E_ν is given by

$$E_\nu = \sqrt{m_\nu^2 + p_\nu^2}, \tag{2.4}$$

a neutrino with non-zero rest mass always takes some of the released energy and hereby reduces the maximal energy E the electron can receive. eq. (2.5) gives the differential rate for an allowed β-decay in dependence of the electron energy E [13]:

$$\frac{\mathrm{d}\Gamma}{\mathrm{d}E} = C \cdot F(Z', E) \cdot p \cdot (E + m_e) \cdot (E_0 - E) \cdot \sqrt{(E_0 - E)^2 - m_\nu^2} \cdot \Theta(E_0 - E - m_\nu). \tag{2.5}$$

[1] We use natural units ($\hbar = c = 1$) for better readability

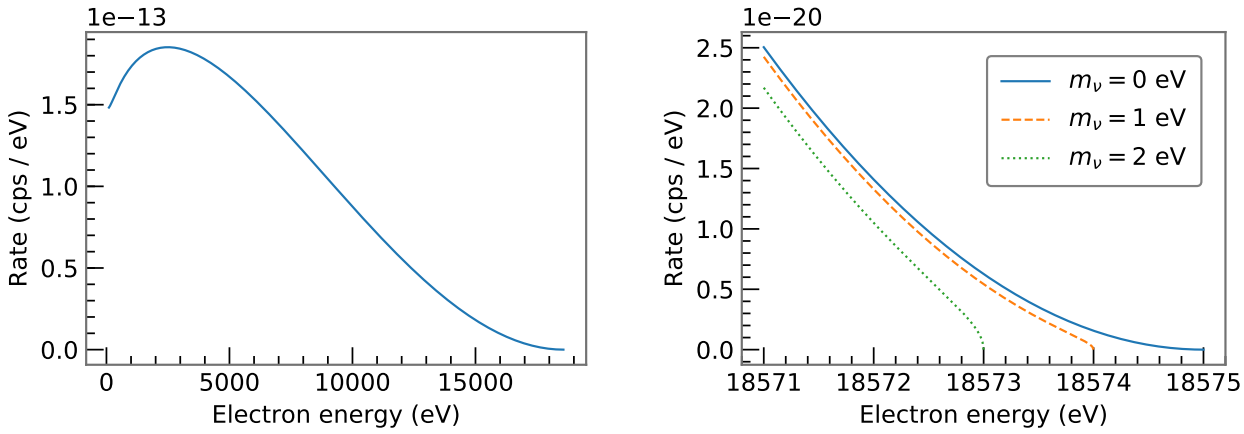

(a) Shape of spectrum in full range.

(b) Impact of non-zero neutrino masses in E_0 region.

Figure 2.1: Differential tritium β-spectrum in dependence of electron energy.

Here the constant

$$C = \frac{G_F^2 \cos^2 \theta_C}{2\pi^3} \cdot |M_{nuc}|^2 \tag{2.6}$$

incorporates the Fermi constant G_F, the Cabbibo angle θ_C and the nuclear matrix element M_{nuc}, $F(Z', E)$ is the Fermi function that accounts for electromagnetic interaction of the outgoing electron with the daughter nucleus and the Heaviside function Θ assures energy conservation. This dependence is shown in fig. 2.1a while the impact of non-zero neutrino masses on the β-spectrum shape in the endpoint region is displayed in fig. 2.1b.

As one can deduce from fig. 2.1b, measuring the differential spectrum in the endpoint region with sub-eV precision is an option to determine the absolute neutrino mass scale. From the magnitude of the impact it is clear that one requires an experiment with excellent energy resolution in the eV range and the very low rates in the endpoint region show that a highly luminous source is needed. Both needs are fulfilled in the KATRIN experiment and are explained in section section 2.3.

2.2 Molecular Tritium as Beta-Decay Source

Tritium as a β-emitter has various advantageous properties for a β-decay experiment [14]:

- Its endpoint value of $E_0 \approx 18.6\,\text{keV}$ [13] is the second lowest of all isotopes undergoing β-decay. A low endpoint value is advantageous as it leads to relatively more counts in the endpoint region in which the neutrino mass manifests itself and for technical reasons as it requires lower voltages in operation of the MAC-E filter described in section 2.3.

- The tritium decay is a super-allowed transition which leads to a rather short half-life of $T_{1/2} = 12.3\,\text{years}$ with correspondingly high rates at low source densities. Additionally the nuclear matrix element is energy independent and easy to calculate.

- In its molecular form T_2, tritium can be used in gaseous state at low temperatures. This state is preferred as systematic uncertainties are decreased and higher rates are achievable.

Since KATRIN uses tritium in its molecular form, tritium β-decay is described by

$$T_2 \rightarrow ({}^3\text{HeT})^+ + e^- + \bar{\nu}_e + Q. \tag{2.7}$$

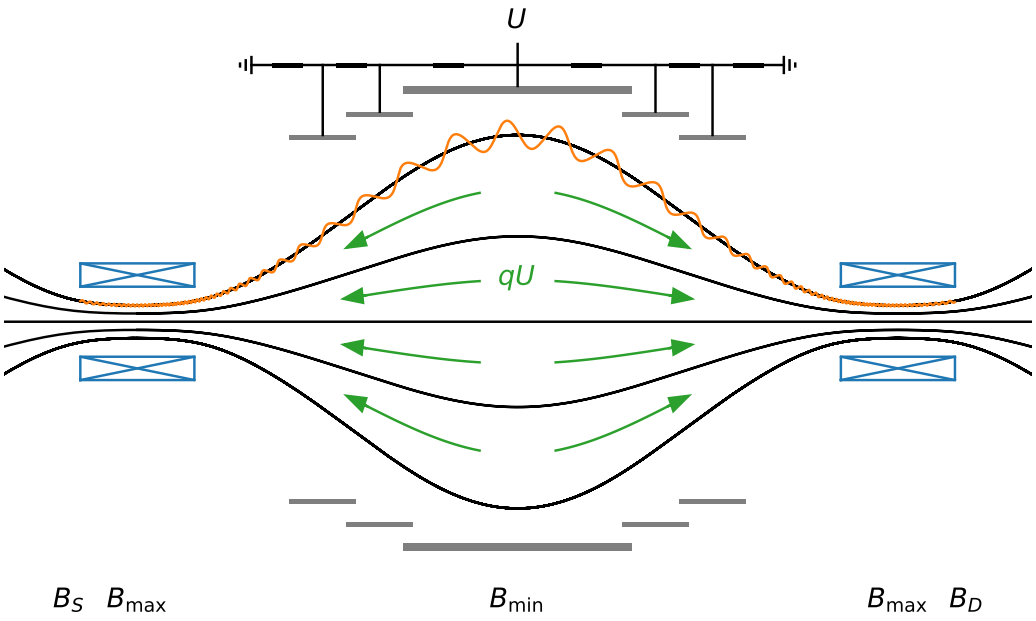

Figure 2.2: Principle of the MAC-E filter, figure adapted from [15].

2.3 Measuring Principle: MAC-E Filter Electron Spectroscopy

The operation principle of KATRIN is an integral measurement of the tritium β-spectrum using magnetic adiabatic collimation (MAC) and an electrostatic (E) high-pass filter. It is depicted in figure 2.2.

Electrons emitted in the source with magnetic field B_{source} are guided along the magnetic field lines towards the center of the spectrometer and perform a cyclotron motion superimposed to their movement along the magnetic field. The magnetic field in the spectrometer B_{ana} is several orders of magnitude smaller which creates a magnetic field gradient. As the magnetic flux $\Phi = B \cdot A$ is constant, the spectrometer must be much larger than the source. Electron momentum perpendicular to the field line $p_\perp$ is transformed into momentum parallel to the field line $p_\parallel$ adiabatically, meaning electron orbital momentum is conserved, along this gradient (shown in orange).

A large voltage U in the order of 18 kV is applied at the minimum magnetic field which creates an electrostatic barrier with energy qU (shown in green). Only electrons with parallel energy $E_\parallel \geq qU$ pass this barrier and are re-accelerated towards the detector leading to the integral measurement of the decay spectrum.

If the source was positioned at maximum magnetic field, all electrons emitted in direction of the spectrometer would be accepted or in other words the accepted solid angle $\frac{\Omega}{4\pi} = \frac{1}{2}$. In practice this is unfavourable as electrons with large starting angles travel long distances in the source which increases their probability to scatter. Therefore the source is placed at a lower magnetic field $B_{\text{source}} < B_{\text{max}}$ leading to a reduced maximum acceptance angle by the magnetic mirror effect of

$$\theta_{\text{max}} = \arcsin \sqrt{\frac{B_{\text{source}}}{B_{\text{max}}}} \tag{2.8}$$

and a correspondingly decreased solid angle of

$$\frac{\Omega}{4\pi} = \frac{1 - \cos\theta_{\text{max}}}{2}. \tag{2.9}$$

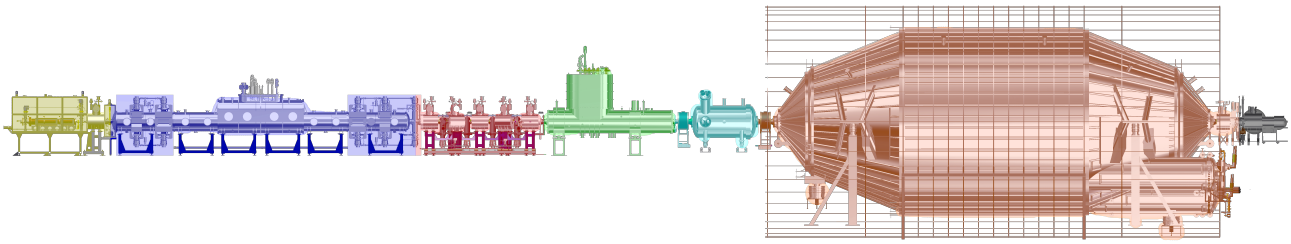

a) b) c) d) e) f) g)

Figure 2.3: Overview of the KATRIN experiment with the main components:
a) Rear section
b) Windowless gaseous tritium source (WGTS)
c) Differential pumping section (DPS)
d) Cryogenic pumping section (CPS)
e) Pre-spectrometer (PS)
f) Main-spectrometer (MS)
g) Focal plane detector (FPD)

2.4 Experimental Setup

An overview of the experimental setup is given in figure 2.3. Each element is briefly described in the following paragraphs.

2.4.1 Rear Section

Main purpose of the rear section is to supply a defined electric potential of the tritium gas in the source by providing a conducting surface, the rear wall. In addition it houses monitoring and calibration tools. [16]

2.4.2 Windowless Gaseous Tritium Source

The windowless gaseous tritium source (WGTS) [17] is an ultra stable and highly luminous gaseous tritium source consisting of a stainless steel tube of $l_S = 10\,\text{m}$ length and $d_S = 90\,\text{mm}$ diameter. Tritium gas of high purity $\epsilon_T \geq 95\,\%$ is continuously injected into the source through more than 250 holes at its centre. The gas then freely streams to both ends and is pumped away by multiple turbo-molecular pumps and then fed into a sophisticated loop system which reprocesses and re-injects the tritium.

To obtain a high tritium density at reasonable pressure and flow rate and to reduce the effects of Doppler broadening, the source is operated at a low temperature of about 30 K.

The number of molecules in the source is described by the column density ρd which is the gas density integrated over the source length. It is related to the total number of tritium atoms in the source by

$$N_{\text{tot}} = 2 \cdot A_S \cdot \rho d \tag{2.10}$$

where the factor two accounts for the number of atoms in a T_2 molecule and A_S is the source area given by

$$A_S = \pi \cdot \left(\frac{d_S}{2}\right)^2 . \tag{2.11}$$

In operation only part of the source area is mapped to the detector to avoid electrons which scattered on the source tube. The effective source area can be retrieved via the magnetic flux and the magnetic field in

the source:

$$A_{\text{eff}} = \frac{\Phi}{B_{\text{source}}}. \tag{2.12}$$

This reduces the effective number of atoms seen to:

$$N_{\text{eff}} = 2 \cdot A_{\text{eff}} \cdot \rho d. \tag{2.13}$$

During the recent KATRIN neutrino mass campaign the magnetic field of the source was $B_{\text{source}} = 2.52\,\text{T}$ and the column density was $\rho d \approx 4.2 \times 10^{21}\,\text{m}^{-2}$. The maximum magnetic field setting $B_{\text{max}} = 4.23\,\text{T}$ leads to the maximum acceptance angle $\theta_{\text{max}} \approx 50.52°$ using (2.8).

2.4.3 Pumping Sections

Tritium from the source may not reach the spectrometers as decay processes in the spectrometers would be a major source of background. The task of the pumping sections is to reduce the tritium flow rate by 14 orders of magnitude in combination with the source which already achieves a reduction by a factor of 100.

A reduction by more than a factor of 10^5 is achieved by the differential pumping section (DPS) [18] which uses turbo-molecular pumps (TMPs). The remaining reduction is achieved by passive adsorption of tritium molecules onto the tube surfaces in the cryogenic pumping section (CPS) [19] operated at a temperature of 4.5 K. These cold surfaces are covered by a thin argon frost layer to enhance the trapping probability of tritium molecules.

Both pumping sections are built in a chicane shape. Electrons are guided adiabatically by magnetic fields through the turns while uncharged molecules hit the wall and are pumped away or adsorbed.

2.4.4 Pre- and Main-Spectrometer

Both the pre- and the main-spectrometer are built following the MAC-E filter principle described in section 2.3.

The smaller pre-spectrometer is operated at a retarding energy of around 300 eV less in absolute value than the main spectrometer. It thus acts as a pre-filter rejecting the majority of uninteresting electrons that would not make it past the main spectrometer for background reduction.

Core of the KATRIN experiment is the large main spectrometer with a diameter of 10 m. Its energy resolution is determined by the magnetic field settings:

$$\frac{\Delta E}{E} = \frac{B_{\text{ana}}}{B_{\text{max}}}. \tag{2.14}$$

For the recent KATRIN tritium campaign the minimum magnetic field in the analysing plane of the main spectrometer was $B_{\text{ana}} = 6 \times 10^{-4}\,\text{T}$ leading to an energy resolution of $\Delta E \approx 2.7\,\text{eV}$ using (2.14) and assuming an electron energy of 18.6 keV.

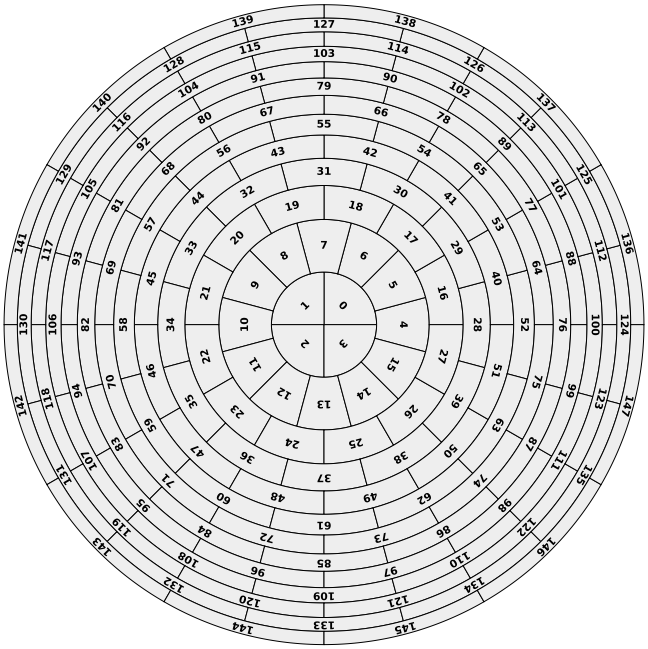

Figure 2.4: Pixel segmentation of the focal plane detector.

2.4.5 Focal Plane Detector

The electrons that pass the main spectrometer are re-accelerated due to the MAC-E filter and further post-acceleration, as high energy electrons are easier to detect and to shift the spectrum above detector-related background, and guided to the focal plane detector (FPD) [20]. The detector is a multi-pixel silicon semiconductor detector with an energy resolution of around 1.4 keV (FWHM) per pixel. The 148 pixels of equal area are arranged in a dart-board shape as shown in figure 2.4. Each pixel counts the number of electrons detected. The radial and azimuthal segmentation allows to correct for inhomogeneities in source, magnetic and electric fields. The efficiency of the detector $\epsilon_{\text{detector}}$ is determined by the region of interest (ROI) cut and physical effects such as back-scattering. Typical values are within 0.9 to 0.95.

2.5 Modelling of the Integrated Beta-Decay Spectrum

This section focusses on deriving a model of the integrated β-decay spectrum describing the expected rate of the KATRIN experiment. First, two effects modifying the differential rate $\frac{\mathrm{d}\Gamma}{\mathrm{d}E}$ are explained. Afterwards the response of the KATRIN setup is discussed and finally these components are combined to a complete model of the rate expectation.

2.5.1 Final State Distribution

As described in section 2.2, KATRIN uses tritium in its molecular form as β-decay source. Therefore the daughter molecule can be in a rotational-vibrational or electronic excited state with energy V_f and corresponding probability P_f. This modifies eq. (2.5) as the effective maximum energy available for electron and neutrino shifts away from the endpoint: $E_0 \to E_0 - V_f$. Introducing $\epsilon_f = E - E_0 - V_f$ the decay rate now reads as

$$\frac{\mathrm{d}\Gamma}{\mathrm{d}E} = C \cdot F(Z', E) \cdot p \cdot (E + m_e) \cdot \sum_f P_f \cdot \epsilon_f \cdot \sqrt{\epsilon_f^2 - m_\nu^2} \cdot \Theta(\epsilon_f - m_\nu). \tag{2.15}$$

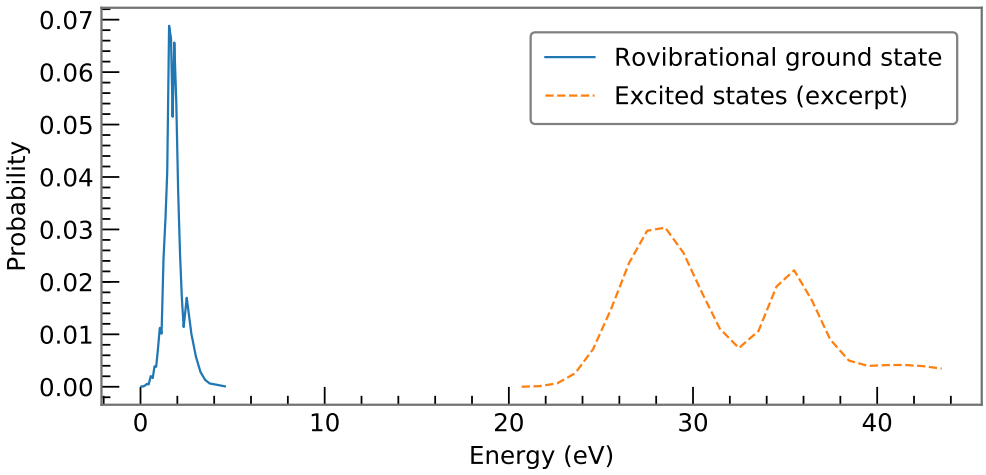

Figure 2.5: Final state distribution of $(^3\mathrm{HeT})^+$ according to A. Saenz et al. [21]. The distribution is split into two parts: the rovibrational ground state (blue) and the excited states (orange).

Precise knowledge of the distribution of these final states is of high importance for neutrino mass measurements as inaccuracies can lead to a biased neutrino mass result. The final state distribution (FSD) can be calculated from theory as done for example by Saenz et al. [21]. An excerpt of the FSD of $(^3\mathrm{HeT})^+$ is shown in fig. 2.5.

It is clearly split into two parts:

- the rovibrational ground state centred at 1.7 eV with a Gaussian width of about 0.36 eV
- and a set of electronic excited states with energies > 20 eV.

2.5.2 Doppler Effect

Additionally, since the tritium molecules in the source are in thermal motion, the differential spectrum is broadened by the Doppler effect. This can be described by convolving the differential spectrum, see eq. (2.15), with a Maxwellian distribution g:

$$\frac{\mathrm{d}\Gamma}{\mathrm{d}E}(E) \to \int_{-\infty}^{\infty} g(E-\epsilon)\frac{\mathrm{d}\Gamma}{\mathrm{d}E}(\epsilon)\,\mathrm{d}\epsilon. \tag{2.16}$$

In its non-relativistic approximation g is described by a normal distribution

$$g(E-\epsilon) = g(\Delta E) = \frac{1}{\sqrt{2\pi}\sigma_E}\cdot\exp\left(-\frac{\Delta E^2}{2\sigma_E^2}\right) \tag{2.17}$$

with the broadening width

$$\sigma_E = \sqrt{2Ek_\mathrm{B}T\frac{m_e}{m_{\mathrm{T}_2}}} \tag{2.18}$$

depending on the energy of the emitted electron E, the Boltzmann constant k_B, the source temperature T and the mass ratio of the electron and T_2. Inserting values typical for the KATRIN experiment, $E = E_0 \approx 18.6\,\mathrm{keV}$, $T = 30\,\mathrm{K}$, leads to a broadening of $\sigma_E = 93.5\,\mathrm{meV}$.

Table 2.1: Scattering probabilities in percent

P_0	P_1	P_2	P_3	P_4	P_5	P_6	P_7	P_8	P_9	P_{10}
44.42	29.58	15.65	6.785	2.487	0.790	0.221	0.056	0.012	0.003	0.001

2.5.3 Response Function

The response function $R(qU, E)$ describes the probability of an electron with energy E to pass the MAC-E filter at a given retarding energy qU. In an ideal apparatus without energy loss it would consist of a simple step function:

$$R(qU, E) = \begin{cases} 0 & E < qU \\ 1 & E \geq qU. \end{cases} \tag{2.19}$$

In the KATRIN experiment two effects dominate the response function: the transmission function of the MAC-E filter and energy loss due to scattering effects in the source.

Not all the perpendicular momentum of an electron is converted to momentum parallel to the electric field in the spectrometer. Therefore also electrons with $E \geq qU$ may not pass the electrostatic barrier. The transmission probability can be described by

$$T(qU, E) = \begin{cases} 0 & E < qU \\ \frac{1-\sqrt{1-f\cdot\frac{B_{\text{source}}}{B_{\text{ana}}}\cdot\frac{E-qU}{E}}}{1-\sqrt{1-\frac{B_{\text{source}}}{B_{\text{max}}}}} & qU \leq E \leq qU\frac{f\cdot B_{\text{max}}}{f\cdot B_{\text{max}}-B_{\text{ana}}} \\ 1 & E > qU\frac{f\cdot B_{\text{max}}}{f\cdot B_{\text{max}}-B_{\text{ana}}} \end{cases} \tag{2.20}$$

with the relativistic factor

$$f = \frac{\frac{E-qU}{m_e}+2}{\frac{E}{m_e}+2}. \tag{2.21}$$

The shape of the transmission function is shown in fig. 2.6a for typical parameter values during the recent neutrino mass measurements.

The major energy loss component is inelastic scattering of electrons with tritium molecules in the source. The probability of an electron to scatter i-times is described by

$$P_i = \frac{1}{1-\cos\theta_{\text{max}}}\int_0^{\theta_{\text{max}}} \sin(\theta)\int_0^1 P_{\text{inel},i}(z,\theta)\,\mathrm{d}z\,\mathrm{d}\theta. \tag{2.22}$$

with the inelastic scattering probability

$$P_{\text{inel},i}(z,\theta) = \frac{(\lambda(z,\theta)\cdot\sigma_{\text{inel}})^i}{i!}\cdot e^{-\lambda(z,\theta)\cdot\sigma_{\text{inel}}},\ \lambda(z,\theta) = \frac{z\cdot\rho d}{\cos\theta} \tag{2.23}$$

assuming no angular change after scattering. The energy-dependent inelastic scattering cross section [22] is given by

$$\sigma_{\text{inel}}(E) = \frac{4\pi a_0^2}{E/R}\left[1.5487\ln\left(\frac{\beta^2}{1-\beta^2}\right)+17.4615\right] \tag{2.24}$$

with the Bohr radius a_0 and the rydberg energy R. The scattering probabilities zero to ten are listed in table 2.1 assuming a column density value of $\rho d = 4.5\times10^{21}\,\mathrm{m}^{-2}$ and an energy $E = 18\,575\,\mathrm{eV}$.

The energy ϵ lost by i-fold scattering can be described by the energy loss function $f_i(\epsilon)$. An electron that does not scatter, loses no energy. Its energy loss function is therefore simply a Dirac δ-function:

$$f_0(\epsilon) = \delta(\epsilon). \tag{2.25}$$

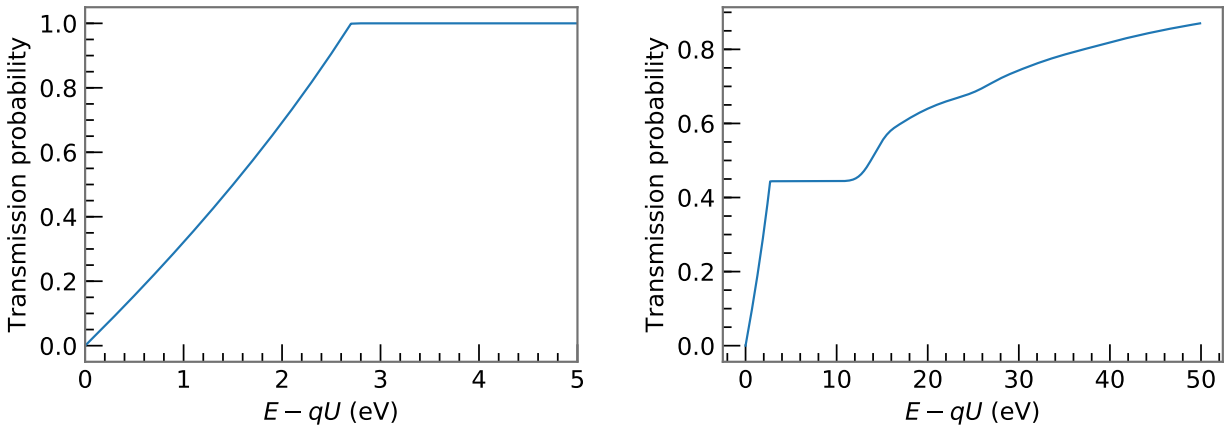

(a) Transmission function

(b) Response function

Figure 2.6: Shape of transmission and response function.

Electrons that scatter once lose energy according to

$$f_1(\epsilon) = \begin{cases} A_1 \cdot \exp\left(-2\left(\frac{\epsilon-\epsilon_1}{\omega_1}\right)^2\right) & \epsilon < \epsilon_C \\ A_2 \cdot \frac{\omega_2^2}{\omega_2^2+4(\epsilon-\epsilon_2)^2} & \epsilon \geq \epsilon_C \end{cases} \tag{2.26}$$

where the Gaussian part comes from excitation processes and the Lorentzian part from ionization of tritium molecules [23, 24]. Energy loss functions for $i \geq 2$ scatterings can be obtained by convolving (2.26) $(i-1)$-times with itself. The energy loss functions for one to four scatterings are displayed in 2.7. This simple analytical energy loss function is not precise enough for KATRIN's design sensitivity. Therefore there will be dedicated electron gun measurements to determine the energy loss function using a deconvolution approach [25].

The total response function is then composed as a convolution of the transmission function with the energy loss function.

$$R(qU,E) = \int_0^{E-qU} T(qU, E-\epsilon) \sum_{i=0}^{\infty} P_i \cdot f_i(\epsilon)\, \mathrm{d}\epsilon \tag{2.27}$$

In practice 5 to 10 scatterings are considered depending on the size of the analysis window. Scattering more often is highly unlikely as can be seen in table 2.1. An example of the response function is shown in figure 2.6b.

2.5.4 Model of the Rate Expectation

As mentioned at the beginning of this chapter, KATRIN measures an integrated tritium β-spectrum. The shape is composed of the differential spectrum $\frac{\mathrm{d}\Gamma}{\mathrm{d}E}(E)$ described in (2.15) and the response function $R(qU,E)$ derived in (2.27):

$$I(qU) = C \cdot \int_{qU}^{E_0} \frac{\mathrm{d}\Gamma}{\mathrm{d}E}(E) \cdot R(qU,E)\, \mathrm{d}E \tag{2.28}$$

with the constant prefactor C

$$C = N_{\mathrm{eff}} \cdot \frac{1-\cos\theta_{\mathrm{max}}}{2} \cdot \epsilon_{\mathrm{detector}} \tag{2.29}$$

consisting of the effective number of tritium atoms in the source N_{eff} (2.13), the solid angle (2.9) and the detector efficiency $\epsilon_{\mathrm{detector}}$.

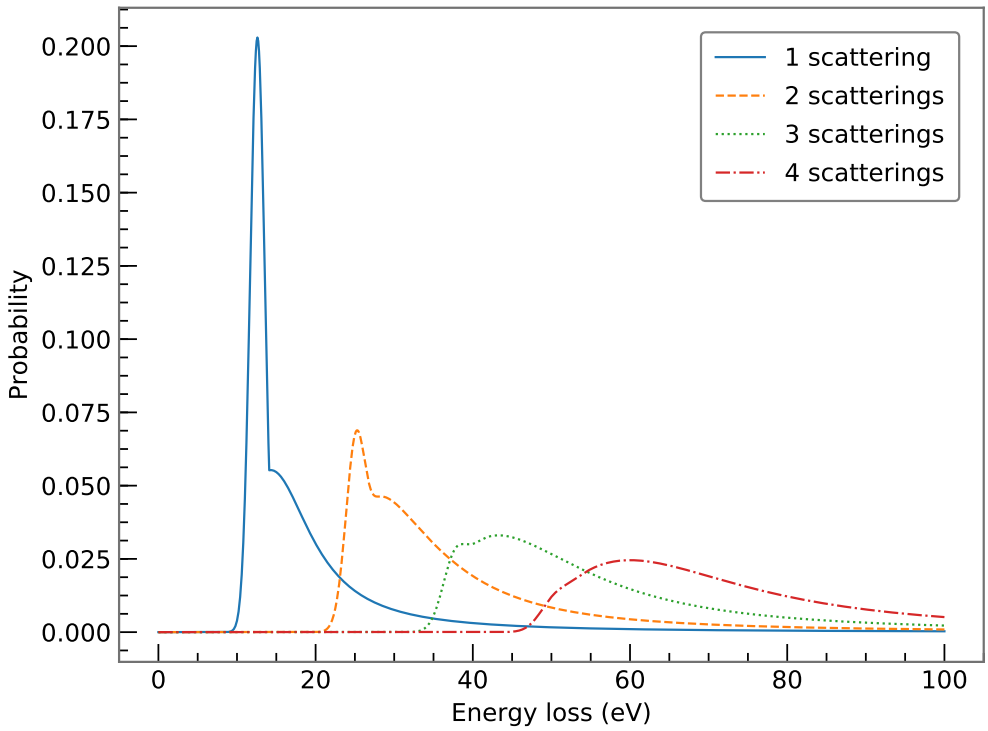

Figure 2.7: Energy loss function according to [23, 24]. The function for 1 scattering (blue) is the representation of (2.26). Higher order functions are retrieved by convolving this function with itself (orange, green, red).

In addition to the signal, a constant background rate B is expected. The total rate is then

$$\Gamma(qU) = I(qU) + B = C \cdot \int_{qU}^{E_0} \frac{\mathrm{d}\Gamma}{\mathrm{d}E}(E) \cdot R(qU, E)\, \mathrm{d}E + B \tag{2.30}$$

Chapter 3

Basic Principles of Data Analysis

In this chapter we will cover some of the basic principles of data analysis. We will make heavy use of these during the lab course, so make sure to read this carefully. In case there are any questions or something is unclear, we can discuss this before starting the actual tasks.

3.1 Maximum Likelihood Analysis

The likelihood function $\mathscr{L}$ is used in statistical methods of parameter inference. It describes how probable a specific outcome of an experiment x is given a model μ. The model itself can depend on a set of parameters $\vec{\theta}$. The likelihood function then reads as

$$\mathscr{L} = \mathscr{L}(\mu(\vec{\theta}); x) = \mathscr{L}(\vec{\theta}; x). \tag{3.1}$$

To retrieve the model that best describes the data, a set of parameters $\vec{\theta}$ is found such that it maximizes the likelihood function.

We now infer the basic likelihood function describing KATRIN data. In KATRIN an integrated tritium β-decay spectrum is measured. As the decay process itself is stochastic, the number of expected decays and hence the number of expected electron counts is described by a probability distribution function (PDF). Assuming the decay rate in the source is constant and the individual decays are independent of one another, the underlying PDF of the number of decays is the Poisson distribution in equation (3.2). It describes the probability to observe N counts given an average model prediction $\mu(\vec{\theta})$:

$$P(N \text{ counts}; \mu(\vec{\theta})) = e^{-\mu(\vec{\theta})} \frac{\mu^N(\vec{\theta})}{N!}. \tag{3.2}$$

Thus $\mathscr{L}(\mu(\vec{\theta}); N) = P(N; \mu(\vec{\theta}))$ is the likelihood function of the parameters $\vec{\theta}$ for a single point of the tritium β-spectrum. The model prediction μ includes the differential tritium spectrum and modelling of the KATRIN apparatus as described in (2.30).

The entire spectrum consists of many counts N_i measured at given different retarding energies qU_i. The individual points are statistically independent and therefore the joint probability distribution P_{total} for the whole spectrum is the product of the individual PDFs

$$P_{\text{total}}(\vec{\mu}; \vec{N}) = \prod_i e^{-\mu_i} \frac{\mu_i^{N_i}}{N_i!}, \tag{3.3}$$

where i runs over all retarding energies and μ_i is defined as $\mu(qU_i; \vec{\theta})$.

In practice it is numerically favorable to minimize $-\ln\mathscr{L}$ instead of maximizing $\mathscr{L}$ as the product of many small numbers quickly leads to numerical difficulties. In addition, taking derivatives of a sum is much easier than taking derivatives of a product.

For large model predictions μ the Poisson distribution asymptotically tends to the normal distribution with mean μ and standard deviation $\sqrt{\mu} \approx \sqrt{N}$:

$$P(N\text{counts}, \mu) = \frac{1}{\sqrt{2\pi N}} e^{-\frac{(N-\mu)^2}{2N}}. \tag{3.4}$$

In this case minimizing $-\ln\mathscr{L}$ is equivalent to the well-known χ^2-minimization:

$$\begin{aligned}
-\ln\mathscr{L}(\vec{\mu};\vec{N}) &= -\ln\left(\prod_i \frac{1}{\sqrt{2\pi N_i}} e^{-\frac{(N_i-\mu_i)^2}{2N_i}}\right) \\
&= -\sum_i \ln\left(\frac{1}{\sqrt{2\pi N_i}} e^{-\frac{(N_i-\mu_i)^2}{2N_i}}\right) \\
&\propto -\sum_i \ln\left(e^{-\frac{(N_i-\mu_i)^2}{2N_i}}\right) \\
&= \sum_i \frac{(N_i-\mu_i)^2}{2N_i} \\
&=: \frac{1}{2}\chi^2(\vec{\mu};\vec{N}).
\end{aligned}$$

In a basic KATRIN model there are four free parameters in $\vec{\theta}$: the neutrino mass squared m_ν^2, the endpoint value E_0, the normalization of the spectrum A_{sig} and the constant background rate B:

$$\mu(qU, t; m_\nu^2, E_0, A_{\text{sig}}, B) = A_{\text{sig}} \cdot t \cdot \int_{qU}^{E_0} \frac{\mathrm{d}\Gamma(E; m_\nu^2, E_0)}{\mathrm{d}E} \cdot R(qU, E)\,\mathrm{d}E + B \cdot t. \tag{3.5}$$

3.2 Interval Estimation

In addition to finding the model parameters that best describe our data, we are also interested in finding an interval that somewhat describes where the values could lie. The most basic description you should already now from the beginners lab course is the 1-σ uncertainty on a parameter value. To retrieve this from a maximum likelihood analysis one can perform a so-called profile likelihood.

Given our best fit with free parameters $\vec{\theta}_{\text{best}}$ has a $-\ln\mathscr{L}$ value of D_{best} and we search for the 1-σ interval of m_ν^2, we:

- define $D(m_\nu^2)$ as $-ln\mathscr{L}$ minimized with respect to $\hat{\theta} = (E_0, A_{\text{sig}}, B)$ for a given fixed value of m_ν^2,
- define $\Delta D(m_\nu^2) = D(m_\nu^2) - D_{\text{best}} \geq 0$
- and search for $\Delta D(m_\nu^2) = \frac{1}{2}$.

This will in general give us two values, one smaller and one larger than our best fit value, see fig. 3.1.

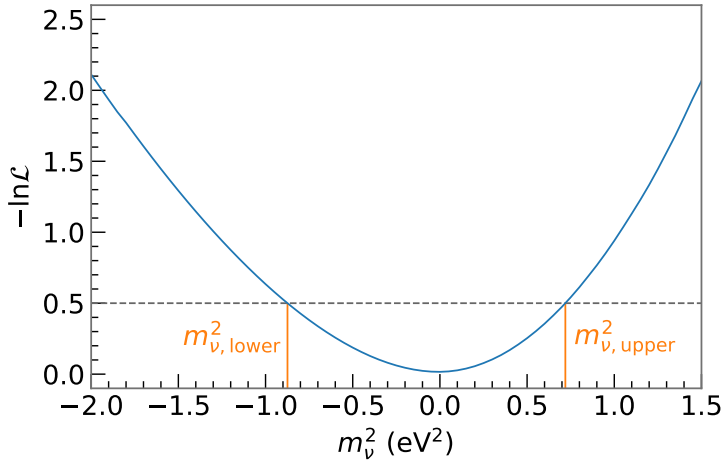

Figure 3.1: Profile likelihood with respect to m^2_ν. We retrieve two values fulfilling $\Delta D = \frac{1}{2}$:
$m^2_{\nu,\text{lower}} = m^2_{\nu,\text{best}} - \sigma_{\text{lower}} < m^2_{\nu,\text{best}} = 0\,\text{eV}^2 < m^2_{\nu,\text{upper}} = m^2_{\nu,\text{best}} + \sigma_{\text{upper}}$.
Often the problems analysed are symmetric and we can simplify to $\sigma = \sigma_{\text{lower}} = \sigma_{\text{upper}}$.

In a frequentist analysis the estimated intervals describe so called confidence intervals. An interval at 90 % confidence level contains the true value in 90 % of the cases. Note that it says nothing about the true value of the one experiment performed. Instead it says if we were to repeat the experiment $N \to \infty$ times, then 90 % of our constructed intervals would contain the true value.

The interval $[m^2_{\nu,\text{lower}}, m^2_{\nu,\text{upper}}]$ which we retrieve from our profile likelihood analysis is given at 1-σ confidence level which corresponds to 68.27 %. If we assume our parameter estimates are normally distributed, which thanks to the central limit theorem is often the case, we can apply scaling factors to come to other common confidence intervals. For example, the 90 % confidence interval is retrieved by multiplying σ with 1.645 and the 95 % confidence interval by multiplying with 1.960.

Chapter 4

Tasks

4.1 Understanding the Model

The following tasks all involve writing your own simple code to see the impact of various parameters on the model relevant for the KATRIN experiment. You can pick any programming language of your choice, but I will only be able to help you in python or C++.

4.1.1 Differential Spectrum

Write your own differential tritium spectrum according to eq. (2.5). You can set the constant prefactor to $C = 1.433\,488 \times 10^{-13}$. You can use the following approximation of the relativistic fermi function:

$$E_{\text{tot}} = E + m_e \qquad \text{total electron energy}$$

$$p = \sqrt{E_{\text{tot}}^2 - m_e^2} \qquad \text{electron momentum}$$

$$\beta = \frac{E_{\text{tot}}}{p} \qquad \text{relativistic beta factor}$$

$$\eta = \frac{2 \cdot \alpha}{\beta} \qquad \text{number of protons in } T_2\text{, fine structure constant } \alpha$$

$$F(Z', E) = \frac{2\pi\eta}{1 - e^{-2\pi\eta}} \cdot (1.002037 - 0.001427\beta).$$

Plot the differential spectrum for $E_0 = 18\,573.7\,\text{eV}$ and different neutrino masses $m_\nu = 0\,\text{eV}$, $1\,\text{eV}$ and $2\,\text{eV}$ in the energy range of $18\,569.7\,\text{eV}$ to $18\,573.7\,\text{eV}$. What happens if you insert a negative value for m_ν^2, for example $m_\nu^2 = -1\,\text{eV}^2$? How could this be interpreted statistically? We can spend some time discussing this, there is no need to have an answer immediately, but we will make use of negative m_ν^2 values later.

4.1.2 Transmission function

Write your own analytical transmission function for the MAC-E filter according to eq. (2.20). For the magnetic fields, use the values $B_{\text{source}} = 2.52\,\text{T}, B_{\text{max}} = 4.23\,\text{T}, B_{\text{ana}} = 6.3 \times 10^{-4}\,\text{T}$. Plot the transmission function for reasonable values of qU and E with respect to the analysis window of KATRIN. What happens if you increase/decrease B_{max}? Or B_{ana}? Relate your observations to the energy resolution of the experiment.

4.1.3 Dummy model

Create your own integral spectrum by integrating the differential spectrum over the transmission function for a given retarding energy:

$$I(qU) = \int_{qU}^{E_0} D(E; m_\nu^2, E_0) \cdot T(qU, E)\, \mathrm{d}E. \tag{4.1}$$

To complete the model, add a constant background term B and multiply your integral spectrum by a signal amplitude A_{sig}:

$$R(qU) = A_{\mathrm{sig}} \cdot I(qU) + B. \tag{4.2}$$

The signal amplitude accounts for the number of tritium molecules in the source, the acceptance angle and other normalization effects. For your dummy model you can use $A_{\mathrm{sig}} = 1$ a.u. Repeat the impact of the neutrino mass plot from section 4.1.1 for a background rate of $B = 200$ mcps[1]. For all plots in this task use the energy range also used later for the analysis, i.e. from 18 535 eV to 18 581 eV. What differences do you observe?

To better understand the impact of the fit parameters on the model, plot:

$$\frac{R_{\mathrm{ref}}(qU) - R_{\mathrm{changed}}(qU)}{R_{\mathrm{ref}}(qU)}. \tag{4.3}$$

As a reference model R_{ref}, use the parameter values $m_\nu^2 = 0\,\mathrm{eV}^2$, $E_0 = 18\,573.7$ eV, $A_{\mathrm{sig}} = 1$ a.u. and $B = 200$ mcps.

Then repeat the plot for the following parameter changes in R_{changed}:

- $m_\nu^2 = 0.5\,\mathrm{eV}^2$
- $m_\nu^2 = 1\,\mathrm{eV}^2$
- $E_0 = 18\,573.6$ eV
- $E_0 = 18\,573.8$ eV
- $A_{\mathrm{sig}} = 0.9$ a.u.
- $A_{\mathrm{sig}} = 1.1$ a.u.
- $B = 190$ mcps
- $B = 210$ mcps

Finally, for the reference model, figure out at which point in retarding energy the signal to background ratio is 1.

What is still missing compared to the complete model described in section 2.5?

[1] cps stands for *counts per second*

4.2 Basics of Data Analysis

For simplification, we will use the differential spectrum with a signal amplitude and a background as model for this section:

$$M(E) = A_{\text{sig}} \cdot \frac{\mathrm{d}\Gamma}{\mathrm{d}E}(E; m_\nu^2, E_0) + B. \tag{4.4}$$

4.2.1 Monte Carlo Data

We now assume some specific points in energy E where we plan to measure our model. In KATRIN, this is called the measuring time distribution (MTD), which describes the points in energy at which we measure and how much relative measuring time is spent there. For simplicity, let's assume 24 points linearly spaced between 18 535 eV to 18 581 eV, each with the same time fraction of $\frac{1}{24}$:

$$\vec{E} = (18535, 18537, 18539, \ldots, 18579, 18581) \tag{4.5}$$

$$\vec{t} = (\frac{1}{24}, \frac{1}{24}, \frac{1}{24}, \ldots, \frac{1}{24}, \frac{1}{24}). \tag{4.6}$$

As a total measurement time, let's assume $t_{\text{tot}} = 750\,\text{d}$. To get the expectation of your model, evaluate it at each point in $\vec{E}$ to retrieve the count rate R and multiply it with the corresponding measuring time $t_{\text{point}} = \frac{t_{\text{tot}}}{24}$ to get the expected number of counts λ. This spectrum, also referred to as the "Asimov spectrum", represents the expectation of the experiment to our best knowledge. Given our parameter values are exactly correct, we will measure one statistical representation of this spectrum. Instead of measuring the exact expectation λ, we will measure random counts N according to the Poisson distribution (see eq. (3.2)).

Thus, to retrieve statistically fluctuated spectra from the Asimov spectrum, plug the expected counts λ into a random Poisson distribution. We will need this later on. To already get a feeling for the fluctuations, generate a few, $\mathcal{O}(10^3)$, of these randomized spectra and plot the standard deviation of each point in E divided by the expected counts over the energy: $\frac{\sigma(E)}{\lambda(E)}$. How does the standard deviation relate to the number of counts? The rate?

4.2.2 Parameter Inference

An important task in data analysis is to retrieve the set of parameter values that best describe the data, see section 3.1. As we have plenty of counts in our example, we will approximate the Poisson distribution by a normal distribution and perform a χ^2 minimization. For a given dataset, you can start with the Asimov spectrum, implement:

$$\chi^2(m_\nu^2, E_0, A_{\text{sig}}, B; \vec{E}, \vec{R}, \vec{\sigma}). \tag{4.7}$$

For the uncertainty $\vec{\sigma}$, use the relation derived in section 4.2.1. Now use your favourite numerical minimizer to minimize the χ^2 function with respect to the fit parameters $m_\nu^2, E_0, A_{\text{sig}}$ and B. Compare the retrieved parameter estimates with the input values you chose. Repeat this for the fluctuated spectra and plot the parameter distributions (histogram) for each of the 4 parameters. What is the mean value of each parameter? What is the standard deviation? Can you give an intuitive explanation of what the mean/standard deviation represents?

4.2.3 Uncertainty and Sensitivity

In addition to the best-fit value, any good physicist is also interested in the uncertainty on this value as described in section 3.2. For this, perform a profile likelihood analysis on the Asimov dataset and retrieve the 1-σ confidence interval for m_ν^2. Convert this into the 90 % confidence interval by applying the appropriate scaling factor. Finally, retrieve the 90 % upper limit of m_ν by calculating $\sqrt{m^2_{\nu,\mathrm{upper}}}$. As we performed this analysis on the Asimov dataset, the one representative to our best knowledge, the intervals calculated correspond to the sensitivity of our experiment.

4.3 Bonus: Analysis of KATRIN Data

In case you still have time and interest, we can now take a look at KATRIN data from the first neutrino mass campaign in spring 2019. The dataset consists of 274 spectral scans, called "runs", each consisting of approximately 2 h of measuring time. To end up with one spectrum to analyse, we sum the counts and average the retarding energies over the 274 runs and over the pixels in the focal plane detector. In the KATRIN jargon, we call this "stacking". This simplification was well-justified for the first measurement campaign as the introduced bias is much smaller than the statistical sensitivity.

We now use one of the software packages to analyse KATRIN data developed here at the Max-Planck-Institute for Physics in Munich. To do so, we have to log-in to one of the Max-Planck PCs and enter a virtual environment:

```
venv fitrium
```

Next we enter the folder with the data:

```
cd Fitting/KNM1/Data
```

The model is configured with a ini configuration file "Fitrium.ini". Let's examine this file together and discuss what the interesting parts mean. Feel free to take notes for your report. Once happy with the model configuration, we can run the fit. The analysis procedure itself is configured using command line flags. The input files are given as positional arguments while any other configurations are optional. The command to run here is:

```
fitrium_fit $(cat included_runs.txt) -u -s -l 18535.5 --identifier my_knm1_fit
```

Let's break this down:

- We pass in all files in the "included_runs.txt" file as positional arguments. These are the data files of the 274 runs.
- We want to sum the counts and average the retarding energies over pixels. In the KATRIN jargon, this is a "uniform" fit. Thus the -u.
- We want to sum the counts and average the retarding energies over runs. In the KATRIN jargon, this is called "stacking". Thus the -s.
- We want to limit our data to all retarding energies $> 18\,535.5\,\mathrm{eV}$. This is done with the -l 18535.5. We do this, as systematic uncertainties grow quickly farther below the endpoint. If we have time, we can discuss this a bit more.

- Finally we give the fit a nice memorable identifier so we can find it in our file system mess later on.

The fit results are now stored in a HDF5 file in the form of fit_*my_knm1_fit.h5. We should also have the most important information, the central value and uncertainties on m_ν^2, printed out on the command line. You should now know what this means and how we got there. Congratulations, you reproduced the most important parts of the first KATRIN neutrino mass publication!

Chapter 5

Report

You should have created a bunch of nice plots during this lab course. For the report:

1. Write a quick introduction to set the frame. There is no need to re-explain all the details of the KATRIN experiment, just a few sentences to explain the bigger picture.

2. Explain the different plots you created, how you got there, and the main message they convey. If there are any questions related to the plot, answer them accordingly. Try to keep some structure and don't simply throw the plots in one after the other.

3. Conclude by mentioning the main things you learned and how you could apply them to other experiments/tasks in experimental physics.

Bibliography

[1] C. L. Cowan Jr. et al. “Detection of the Free Neutrino: A Confirmation”. In: *Science* 124 (1956), pp. 103–104. DOI: 10.1126/science.124.3212.103.

[2] Y. Fukuda et al. “Evidence for Oscillation of Atmospheric Neutrinos”. In: *Phys. Rev. Lett.* 81 (8 1998), pp. 1562–1567. DOI: 10.1103/PhysRevLett.81.1562. URL: https://link.aps.org/doi/10.1103/PhysRevLett.81.1562.

[3] Q. R. Ahmad et al. “Direct Evidence for Neutrino Flavor Transformation from Neutral-Current Interactions in the Sudbury Neutrino Observatory”. In: *Phys. Rev. Lett.* 89 (1 2002), p. 011301. DOI: 10.1103/PhysRevLett.89.011301. URL: https://link.aps.org/doi/10.1103/PhysRevLett.89.011301.

[4] S. Abe et al. “Precision Measurement of Neutrino Oscillation Parameters with KamLAND”. In: *Phys. Rev. Lett.* 100 (22 2008), p. 221803. DOI: 10.1103/PhysRevLett.100.221803. URL: https://link.aps.org/doi/10.1103/PhysRevLett.100.221803.

[5] B. Pontecorvo. “Mesonium and anti-mesonium”. In: *Sov. Phys. JETP* 6 (1957). [Zh. Eksp. Teor. Fiz.33,549(1957)], p. 429.

[6] Ziro Maki, Masami Nakagawa, and Shoichi Sakata. “Remarks on the Unified Model of Elementary Particles”. In: *Progress of Theoretical Physics* 28.5 (1962), pp. 870–880. DOI: 10.1143/PTP.28.870. eprint: /oup/backfile/content_public/journal/ptp/28/5/10.1143/ptp.28.870/2/28-5-870.pdf. URL: http://dx.doi.org/10.1143/PTP.28.870.

[7] Steen Hannestad. “Neutrino physics from precision cosmology”. In: *Progress in Particle and Nuclear Physics* 65.2 (2010), pp. 185–208. ISSN: 0146-6410. DOI: https://doi.org/10.1016/j.ppnp.2010.07.001. URL: http://www.sciencedirect.com/science/article/pii/S0146641010000499.

[8] Steven R. Elliott and Petr Vogel. “DOUBLE BETA DECAY”. In: *Annual Review of Nuclear and Particle Science* 52.1 (2002), pp. 115–151. DOI: 10.1146/annurev.nucl.52.050102.090641. URL: https://doi.org/10.1146/annurev.nucl.52.050102.090641.

[9] Ch Kraus et al. “Final results from phase II of the Mainz neutrino mass search in tritium β decay”. In: *The European Physical Journal C - Particles and Fields* 40.4 (2005), pp. 447–468. ISSN: 1434-6052. DOI: 10.1140/epjc/s2005-02139-7. URL: https://doi.org/10.1140/epjc/s2005-02139-7.

[10] V. N. Aseev et al. “Upper limit on the electron antineutrino mass from the Troitsk experiment”. In: *Phys. Rev. D* 84 (11 2011), p. 112003. DOI: 10.1103/PhysRevD.84.112003. URL: https://link.aps.org/doi/10.1103/PhysRevD.84.112003.

[11] KATRIN Collaboration and KATRIN Collaboration. *KATRIN design report 2004*. Tech. rep. 51.54.01; LK 01; Auch: NPI ASCR Rez EXP-01/2005; MS-KP-0501. Forschungszentrum, Karlsruhe, 2005. 245 pp.

[12] M. Kleesiek et al. *β-Decay Spectrum, Response Function and Statistical Model for Neutrino Mass Measurements with the KATRIN Experiment*. 2018. eprint: arXiv:1806.00369.

[13] E W Otten and C Weinheimer. “Neutrino mass limit from tritium β decay”. In: *Reports on Progress in Physics* 71.8 (2008), p. 086201. URL: http://stacks.iop.org/0034-4885/71/i=8/a=086201.

[14] Susanne Mertens. “Study of Background Processes in the Electrostatic Spectrometers of the KATRIN Experiment”. PhD thesis. 2012.

[15] Martin Slezák. “Monitoring of the energy scale in the KATRIN neutrino experiment”. PhD thesis. Charles University in Prague, 2015. URL: http://www.katrin.kit.edu/publikationen/phd-Martin_Slezak.pdf.

[16] Martin Babutzka. “Design and development for the Rearsection of the KATRIN experiment”. PhD thesis. 2014.

[17] Florian Heizmann, Hendrik Seitz-Moskaliuk, and KATRIN collaboration. “The Windowless Gaseous Tritium Source (WGTS) of the KATRIN experiment”. In: *Journal of Physics: Conference Series* 888.1 (2017), p. 012071. URL: http://stacks.iop.org/1742-6596/888/i=1/a=012071.

[18] S. Lukić et al. “Measurement of the gas-flow reduction factor of the KATRIN DPS2-F differential pumping section”. In: *Vacuum* 86.8 (2012), pp. 1126–1133. ISSN: 0042-207X. DOI: https://doi.org/10.1016/j.vacuum.2011.10.017. URL: http://www.sciencedirect.com/science/article/pii/S0042207X11003800.

[19] W. Gil et al. “The Cryogenic Pumping Section of the KATRIN Experiment”. In: *IEEE Transactions on Applied Superconductivity* 20.3 (June 2010), pp. 316–319. ISSN: 1051-8223. DOI: 10.1109/TASC.2009.2038581.

[20] J.F. Amsbaugh et al. “Focal-plane detector system for the KATRIN experiment”. In: *Nuclear Instruments and Methods in Physics Research Section A: Accelerators, Spectrometers, Detectors and Associated Equipment* 778 (2015), pp. 40–60. ISSN: 0168-9002. DOI: https://doi.org/10.1016/j.nima.2014.12.116. URL: http://www.sciencedirect.com/science/article/pii/S0168900215000236.

[21] Alejandro Saenz, Svante Jonsell, and Piotr Froelich. “Improved Molecular Final-State Distribution of HeT^+ for the β-Decay Process of T_2”. In: *Phys. Rev. Lett.* 84 (2 2000), pp. 242–245. DOI: 10.1103/PhysRevLett.84.242. URL: https://link.aps.org/doi/10.1103/PhysRevLett.84.242.

[22] J. W. Liu. “Total Inelastic Cross Section for Collisions of H_2 with Fast Charged Particles”. In: *Phys. Rev. A* 7 (1 1973), pp. 103–109. DOI: 10.1103/PhysRevA.7.103. URL: https://link.aps.org/doi/10.1103/PhysRevA.7.103.

[23] V.N. Aseev et al. “Energy loss of 18 keV electrons in gaseous T and quench condensed D films”. In: *The European Physical Journal D - Atomic, Molecular, Optical and Plasma Physics* 10.1 (2000), pp. 39–52. ISSN: 1434-6079. DOI: 10.1007/s100530050525. URL: https://doi.org/10.1007/s100530050525.

[24] D. N. Abdurashitov et al. “Electron scattering on hydrogen and deuterium molecules at 14–25 keV by the “Troitsk nu-mass” experiment”. In: *Physics of Particles and Nuclei Letters* 14.6 (2017), pp. 892–899. ISSN: 1531-8567. DOI: 10.1134/S1547477117060024. URL: https://doi.org/10.1134/S1547477117060024.

[25] V. Hannen et al. “Deconvolution of the energy loss function of the KATRIN experiment”. In: *Astroparticle Physics* 89 (2017), pp. 30–38. ISSN: 0927-6505. DOI: https://doi.org/10.1016/j.astropartphys.2017.01.010. URL: http://www.sciencedirect.com/science/article/pii/S0927650517300348.